National Institute of Metrology (Thailand)

Report on APMP Supplementary Comparison
High precision roundness measurement

APMP.L-S4

Final report

J. Buajarern, National Institute of Metrology (Thailand) (NIMT), Thailand

K. Naoi, National Metrology Institute of Japan (NMIJ), Japan

A. Baker, National Measurement Institute (NMIA), Australia

X. Zi, National Institute of Metrology (NIM), China

C. L. Tsai, Center for Measurement Standards / Industrial Technology Research Institute (CMS/ITRI), Taiwan

T. B. Eom, Korea Research Institute of Standards and Science (KRISS), Rep. of Korea

S.L.Tan, National Metrology Centre, Agency for Science, Technology and Research (NMC/A*STAR), Singapore

O. Kruger, National Metrology Institute of South Africa (NMISA), South Africa

November, 2015

Contents

1 Document control

Version Draft B.1	Issued on April 2015.
Version Draft B.2	Issued on July 2015, comments participants taken in to account.
Version Draft B.3	Issued on August 2015, minor editorial change.
Final report	Issued on November 2015, taking into account comments from CCL WG-MRA reviewers

2 Introduction

The broad objective of the Asia Pacific Metrology Program (APMP) is to improve the measurement capabilities in the Asia Pacific region by sharing facilities and experience in metrology. Comparison of calibrations by different laboratories on given artifacts adds confidence in the measurement of standards and leads to international acceptance of the measurements carried out by these laboratories. This intercomparison concerns the calibration of glass hemisphere and roundness assessment of the softgauge.

Standards circulated to all laboratories consist of:

- Two (2) glass hemispheres

- Two (2) softgauges

Measurement conditions for each standard are described in the appropriate section of this document. If the ISO guidelines cannot be followed an approximation may be made with detailed description of how the measurement conditions have varied.

3 Organization

3.1 Pilot and Coordinating Laboratory

The project was piloted by:

Dr Jariya Buajarern

Dimensional Metrology Department, National Institute of Metrology (Thailand)

The pilot laboratory was responsible for

- Preparing the protocol
- Planning the program and organizing the schedule
- Maintaining a list of participants' information
- Liaising with participants
- Collecting and assessing results by accepted statistical methods
- Preparing the draft report
- Distributing the draft report for comment
- Reviewing comments and completing the final report

And the project was coordinated by:

Dr Kazuya Naoi

National Institute of Advanced Industrial Science and Technology (AIST)

The program coordinator was responsible for

- Reviewing the protocol
- Preparing the artifacts
- Declaring the value of the artifacts
- Making initial and final measurements
- Perform stability check of the artifacts
- Reviewing comments and completing the final report

3.2 Participants

The participant information is listed in Table 1.

Table 1. Participant informations.

Laboratory Code	Contact person, Laboratory	Phone, Fax, email
NIMT	Dr Jariya Buajarern National Institute of Metrology (Thailand), NIMT 3/4-5 Moo 3, Klong 5, Klong Luang, Pathumthani 12120, Thailand	Tel. +66 2577 5100 e-mail: jariya@nimt.or.th
NMIJ	Dr Kazuya Naoi National Metrology Institute of Japan, NMIJ National Institute of Advanced Industrial Science and Technology (AIST) Tsukuba Central 3, 1-1-1 Umezono, Tsukuba, Ibaraki 305-8563, Japan	Tel. +81 298614041 e-mail: naoi.k@aist.go.jp
NMIA	Mr Andrew Baker National Metrology Institute, NMIA Department of Industry, Innovation, Science, Research and Tertiary Education Unit 1 - 153 Bertie Street, Port Melbourne, Victoria 3207, Australia	Tel. +61 3 9644 4902 e-mail: andrew.baker@measurement.gov.au
NIM	Dr Xue Zi National Institute of Metrology, NIM Beisanhuandonglu 18, Beijing 100013, China	Tel. +86 1064524915 e-mail: xuez@nim.ac.cn
CMS/ITRI	Mr Chin-Lung Tsai Center for Measurement Standards / Industrial Technology Research Institute (CMS/ITRI) 321 Kuang Fu Rd., Sec. 2, Bldg. 16 30042 Hsinchu, Taiwan	Tel. +886 35743764 e-mail: walter_tsai@itri.org.tw
KRISS	Dr Tae Bong Eom Korea Research Institute of Standards and Science, KRISS 267 Gajeong-Ro, Yuseong-Gu, Daejeon 305-340, Rep. of Korea	Tel. +82 8685100 e-mail: tbeom@kriss.re.kr
NMC/A*STAR	Ms Tan Siew Leng National Metrology Centre/Agency for Science, Technology and Research , NMC/A*STAR 1 Science Park Drive, Singapore 118221	Tel. +65 62791938 e-mail: tan_siew_leng@nmc.a-star.edu.sg
NMISA	Mr Oelof Kruger National Metrology Institute of South Africa, NMISA Private Bag X34, Lynnwood Ridge, Pretoria, 0040, South Africa	Tel. +27 128414340 e-mail: oakruger@nmisa.org

3.3 Schedule

The program is to commence in 2012 with measurement at the coordinating laboratory. The order for measurement is listed in Table 2. Each laboratory was expected to make all required measurement in a two week period and allow a further two week period for transferring the artifacts to the next listed laboratory. Those scheduled for December or January were allowed four weeks for measurement due to expected public holidays and a further two week period for transfer. NMIJ performed measurement 3 times in order to investigate stability of the artifacts. Only the first measurement results from the NMIJ (coordinating laboratory) was included and analyzed.

Table 2. Schedule of the comparison.

Laboratory	**Original schedule**	**Date of measurement**	**Results received**
NMIJ-1	March 2012	March 2012	April 2012
NIMT	April 2012	April 2012	June 2012
NMIA	May 2012	May 2012	August 2012
NMISA	June 2012	June 2012	November 2012
NMC/A*STAR	July 2012	October 2012	May 2013
KRISS	September 2012	November 2012	August 2013
NIMT	October 2012	December 2012	January 2013
NMIJ-2	November 2012	February 2013	Stability check
CMS/ITRI	December 2012	March 2013	August 2013
NIM	January 2013	April 2013	June 2013
NMIJ-3	February 2013	May 2013	Stability check

4 Artefacts

4.1 Description of artefacts

The artifacts to be circulated for assessment of roundness are:

Table 3. List of artefacts.

Identification	Type	Manufacturer
8726	Glass hemisphere	Taylor Hobson
6767		Taylor Hobson
SoftgaugeI	Softgauge	NA
SoftgaugeII		NA

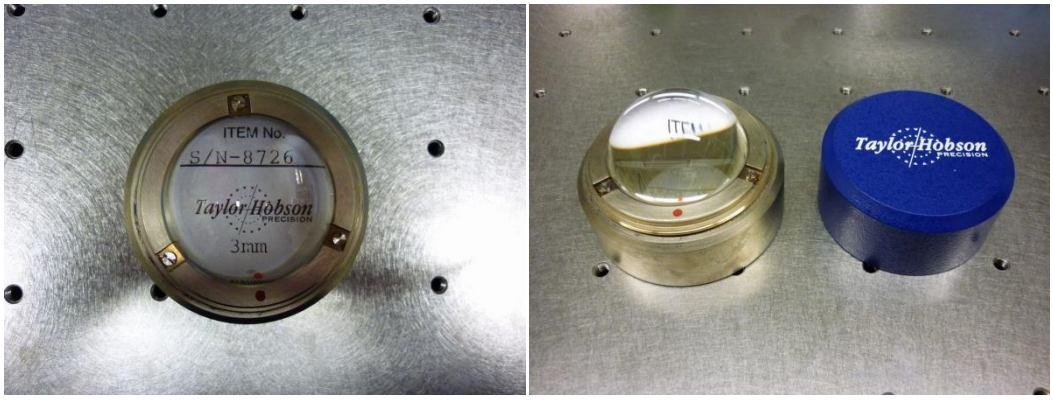

Figure 1. Glass Hemisphere (8726)

Figure 2. Glass Hemisphere (6767)

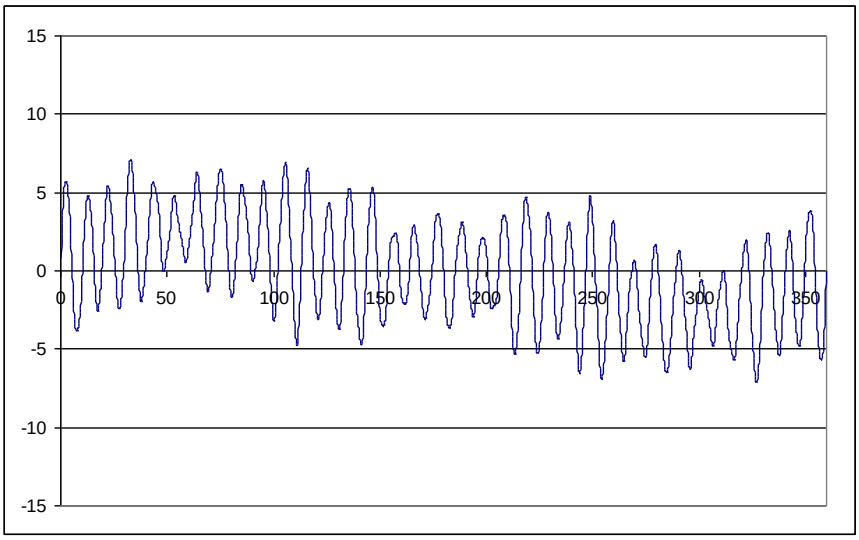

Figure 3. Softgauge I

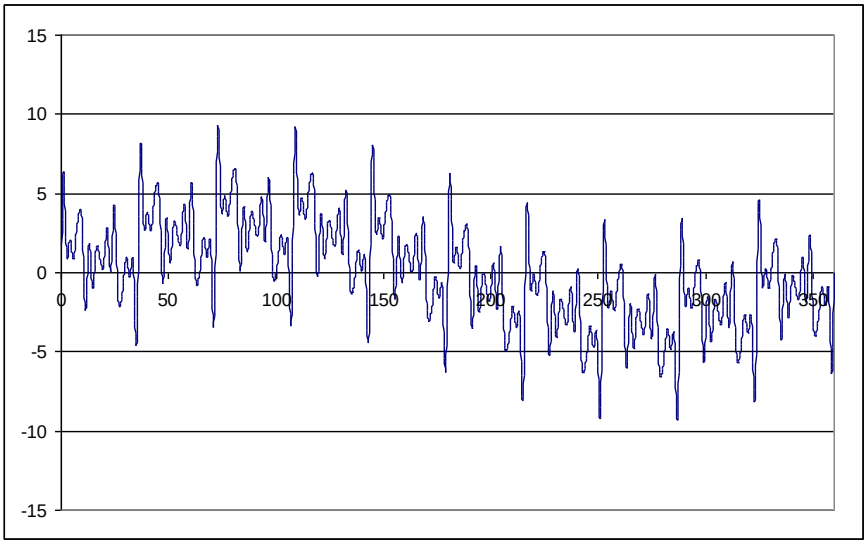

Figure 4. Softgauge II

4.2 Stability of artefacts

The glass hemispheres were measured three times by the co-ordinate laboratory, at the dates indicated in the graphs. The following diagrams show the measured roundness with the stated uncertainties (k=1) after being filtered by 1-50 UPR filter. The observed deviation is much smaller than the standard uncertainty of the measurement which show good stability of the artifacts.

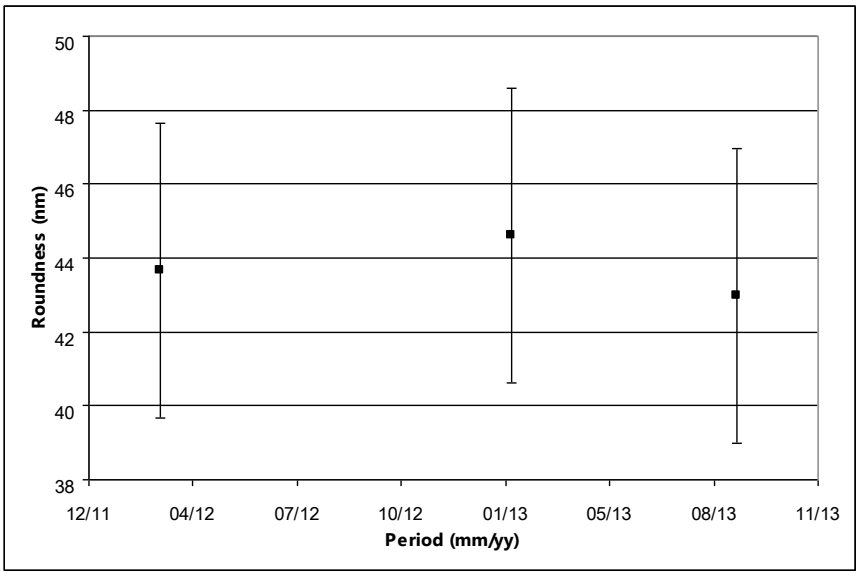

Figure 5. Stability of glass hemisphere (8726) during comparison. Uncertainty bars show standard uncertainty (*k*=1).

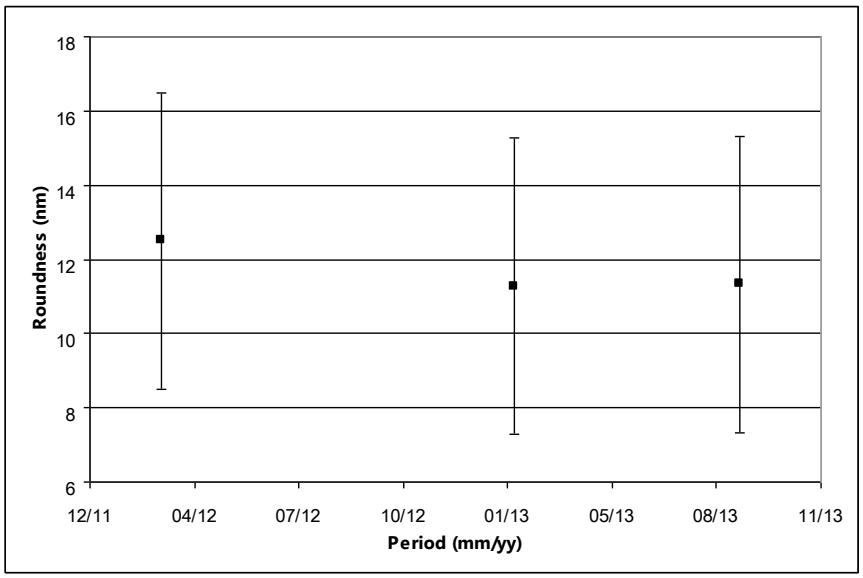

Figure 6. Stability of glass hemisphere (6767) during comparison. Uncertainty bars show standard uncertainty (*k*=1).

5 Measuring instructions

5.1 Measurands

The measurand is the peak to valley roundness deviation with respect to LS reference circle according to ISO/TS 12181-1, filtered at 1-15 UPR and 1-50 UPR with a Gauss filter or 2CR filter.

5.2 Measurement method

To ensure the best possible comparison, measurement are to be performed according to ISO/TS 12181-1 [1] and ISO/TS 12181-2 [2] year 2003.

For glass Hemisphere, the reference mark (red dot on the mount) should be aligned with the 270° reference position of the rotating element. The plane of measurement is 3 mm above the top of the mount as shown in Figure 7.

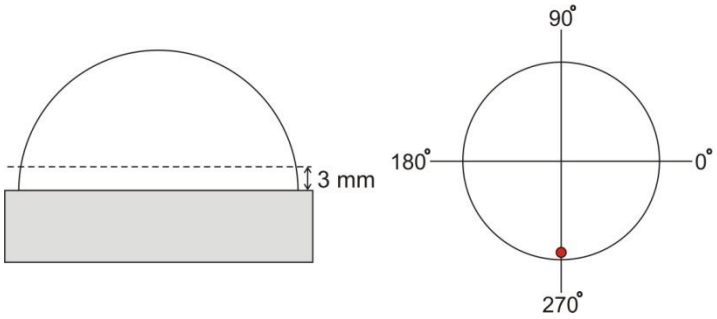

Figure 7: Measurement plane and alignment of the glass hemisphere.

6 Equipment and measuring methods

An overview of the equipment and the measuring methods used is given in Table 4. The conditions which determine the final uncertainty are the spindle repeatability, the probe repeatability, the probe linearity, the method used to calibrate the probe and the method used to compensate for spindle errors. All instruments were equipped with an inductive transducer with a lever-type stylus. The calibration of the probe was generally made directly, or indirectly by means of various transfer standards (piezo-actuators, flick-standards, gauge blocks), referenced to a laser interferometer. The multi-step method was used for compensation of spindle errors. Numbers of steps varied from 10 steps to 20 steps.

Table 4. Measuring instruments and conditions.

Laboratory	Instrument	Error separation	Tip	Measuring force	Point/rev.	$U_{95\%}$ (nm)
NMIJ	Talyrond 73	Multi-step 20 steps	hatchet, radius 6.4 mm	25 mN	2,000	8
NIMT	Talyrond 73	Multi-step 10 steps	hatchet, radius 6.4 mm	5 mN	2,000	8
NMIA	Talyrond 73	Multi-step 12 steps	Tungsten carbide, diameter 1.59 mm	< 8 mN	3,600	10
NMISA	Talyrond 73	Multi-step 12 steps	hatchet, radius 1.5 mm	20 mN	720	15
NMC/A*STAR	Talyrond 395	Multi-step 12 steps	ruby ball, 2 mm	49 mN	3,600	7
KRISS	Talyrond 73	Multi-step 10 steps	Tungsten carbide, radiu 6 mm	Not specified	2,000	7
CMS/ITRI	Talyrond 73	Multi-step 10 steps	hatchet, radius 6.4 mm	< 0.15 N	2,000	8
NIM	Talyrond 73	Multi-step 10 steps	Not specified	Not specified	2,048	6

7 Measurement results

The supplementary comparison reference values (SCRV) were calculated for each artifact using the weighted mean. To each result (x_i) a normalized weight, w_i, was attributed, given by:

$$w_i = C \cdot \frac{1}{[u(x_i)]^2} \tag{1}$$

where the normalizing factor, C, is given by:

$$C = \frac{1}{\sum_{i=1}^{N}\left(\frac{1}{u(x_i)}\right)^2} \tag{2}$$

The weighted mean $\bar{x}_w$ is given by:

$$\bar{x}_w = \sum_{i=1}^{N} w_i \cdot x_i \tag{3}$$

and the uncertainty of the weighted mean is calculated by:

$$u(\bar{x}_w) = \sqrt{\frac{1}{\sum_{i=1}^{N}\left(\frac{1}{u(x_i)}\right)^2}} = \sqrt{C} \tag{4}$$

For the determination of the SCRV, statistical consistency of the results contributing to the SCRV is required. A check for statistical consistency of the results with their associated uncertainties can be made by the Birge ratio, R_B, which compares the observed spread of the results with the expected spread from the individual reported uncertainties.

The Birge ratio is defined as

$$R_B = \frac{u_{ext}\left(\bar{x}_w\right)}{u\left(\bar{x}_w\right)} \tag{5}$$

where $u_{ext}\left(\bar{x}_w\right)$ is the external standard deviation

$$u_{ext}\left(\bar{x}_w\right) = \sqrt{\frac{1}{(N-1)} \cdot \frac{\sum_{i=1}^{N} w_i \left(x_i - \bar{x}_w\right)^2}{\sum_{i=1}^{N} w_i}} \tag{6}$$

The data in a comparison are consistent provided that

$$R_B < \sqrt{1+\sqrt{\frac{8}{N-1}}} \tag{7}$$

where N is the number of laboratories.

For each laboratory's result, the E_n value is calculated. E_n is defined as the ratio of the deviation from the weighted mean, divided by the expanded uncertainty of this deviation.

$$En = \frac{\left|x_i - \bar{x}_w\right|}{\sqrt{U^2\left(x_i\right) - U^2\left(\bar{x}_w\right)}} \tag{8}$$

7.1 Glass hemispheres

7.1.1 Form profile

The data submitted by each participant were filtered with a Gaussian 1-15 UPR and 1-50 UPR except the data from KRISS that were filtered with a 2CR filter. Moreover, NMISA can perform filtering only with a Gaussian 1-50 UPR. Graphical results from all NMIs are shown below.

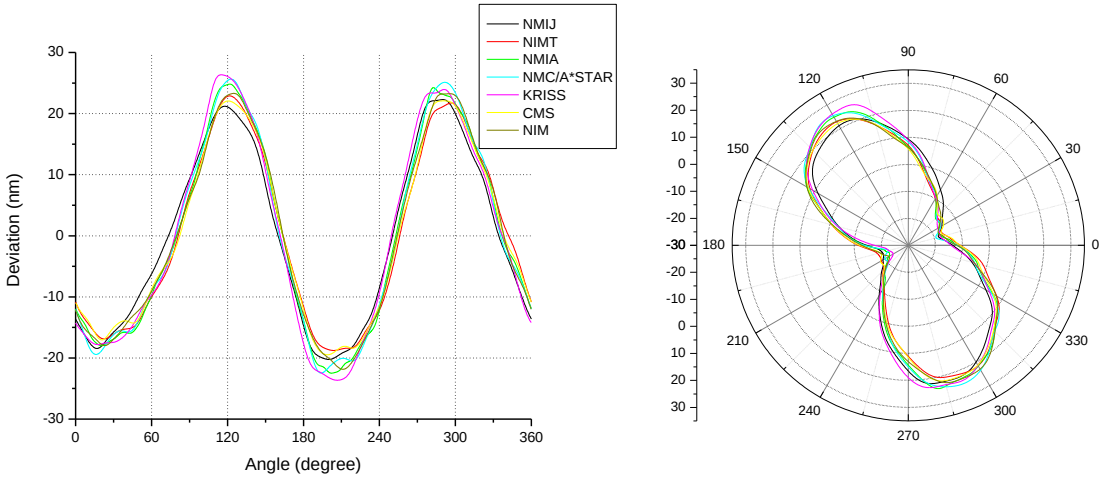

Figure 8: Roundness profile of glass hemisphere SN 8726 at 1-15 UPR.

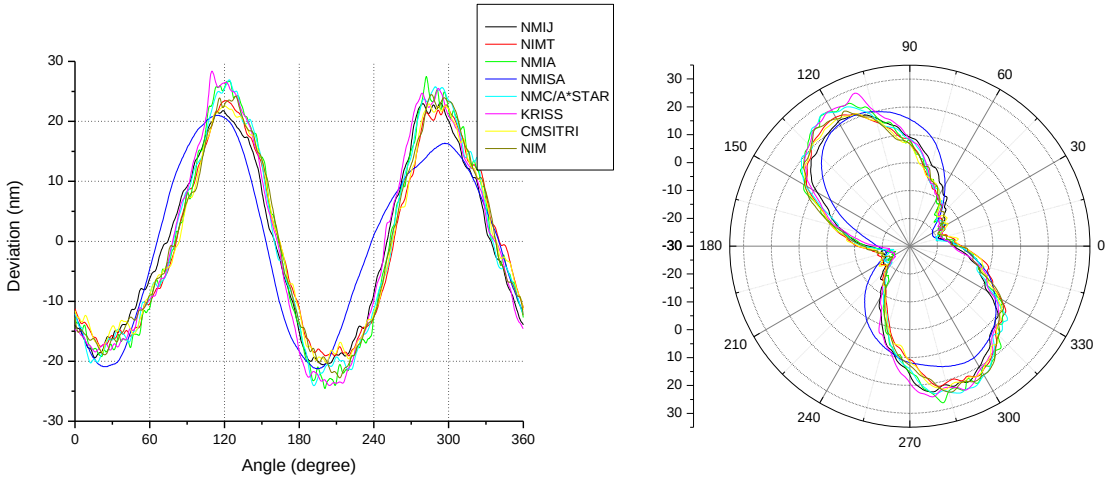

Figure 9: Roundness profile of glass hemisphere SN 8726 at 1-50 UPR.

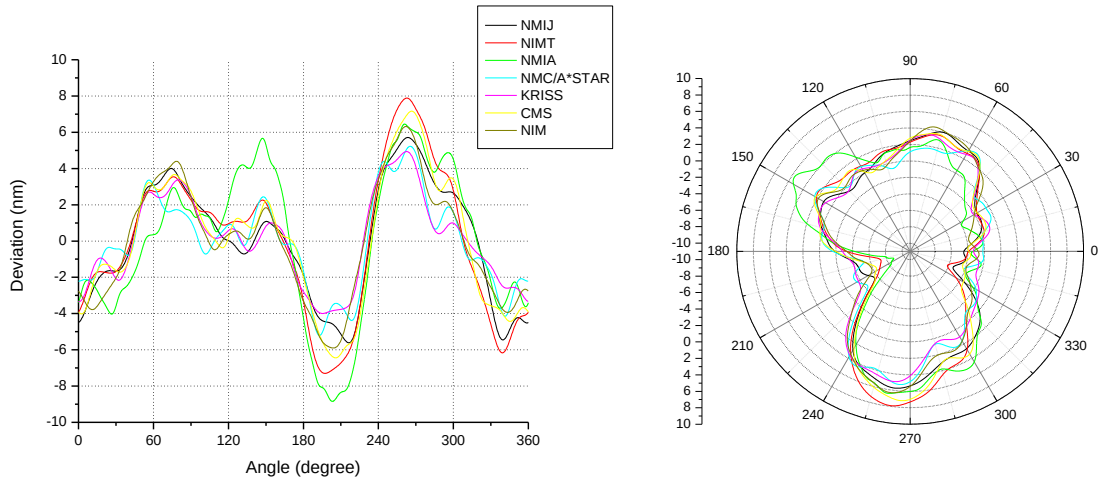

Figure 10: Roundness profile of glass hemisphere SN 6767 at 1-15 UPR.

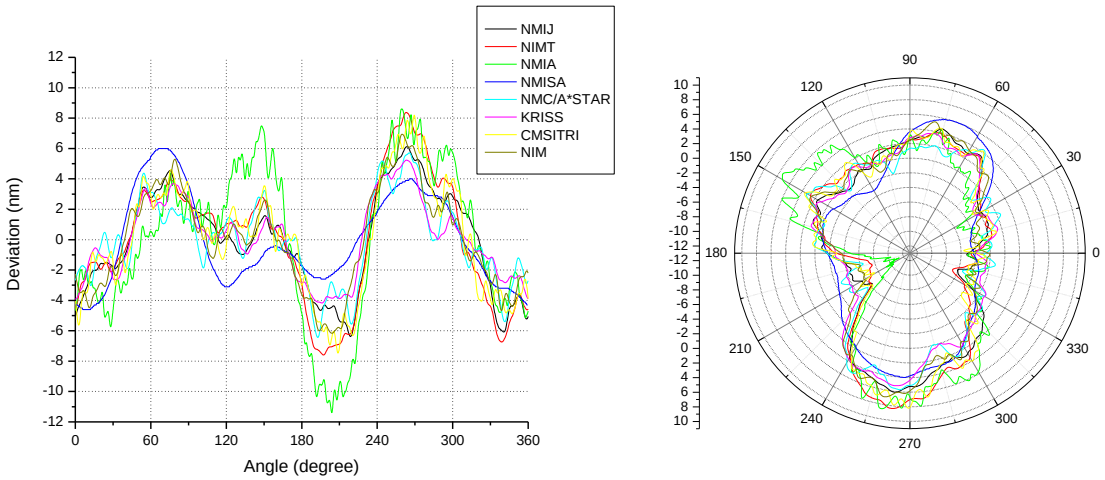

Figure 11: Roundness profile of glass hemisphere SN 6767 at 1-50 UPR.

7.1.2 Numerical result

UPR (Undulations Per Revolution) filter was referred to the least-squares circle (LSC). The following tables list the measurement results submitted by the participants. Each table show the reported results, En values (coverage factor k = 2), weighted mean and Birge ratio (Rb). As NMISA reported only result after a 1-50 UPR Gaussian filtering, result for a 1-15 UPR Gaussian filtering of the NMISA is left blank and did not taken into account for En and Rb calculations.

Table 5. Roundness deviation of glass hemisphere SN 8726 in nm.

Lab	1-15 UPR		1-50 UPR		En	
	LSC	U (k =2)	LSC	U (k =2)	1-15 UPR	1-50 UPR
Weighted mean	45.060	3.18	47.020	3.24	-	-
NMIJ-1	43.0	7.7	44.2	8.0	0.29	0.39
NIMT	41.7	8.0	42.6	8.0	0.46	0.60
NMIA	47.0	10.0	52.0	10.0	0.20	0.53
NMISA	-	-	42.3	15.0	-	0.32
NMC/A*STAR	48.0	9.0	52.0	10.0	0.35	0.53
KRISS	50.0	8.0	52.4	8.0	0.67	0.73
CMS/ITRI	41.5	8.9	43.0	11.0	0.43	0.38
NIM	45.0	8.0	46.0	8.0	0.01	0.14
Rb	0.789	-	0.964	-	-	-
Rb (limit)	1.468	-	1.438	-	-	-

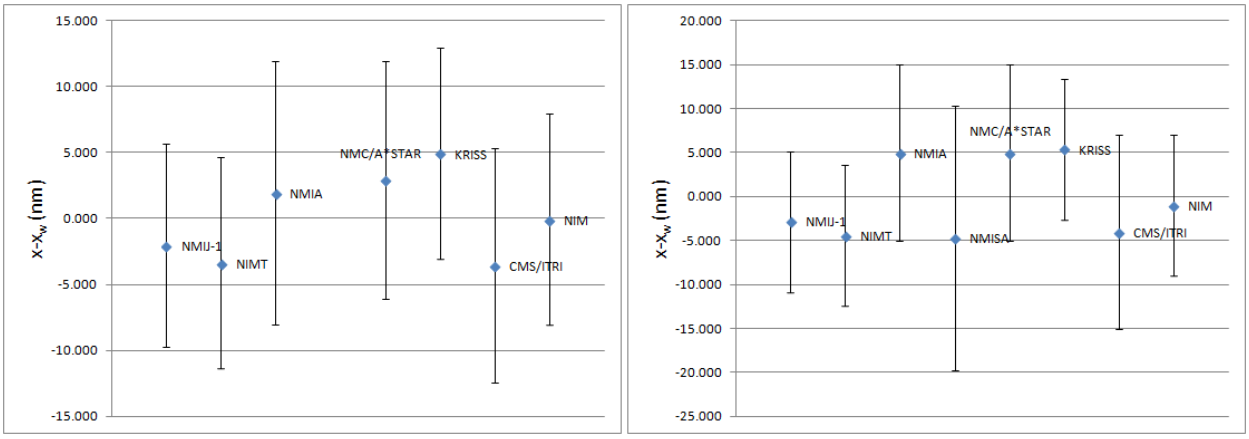

Figure 12: Deviation from SCRV for glass hemisphere SN 8726 at 1-15 UPR and 1-50 UPR.

Table 6. Roundness deviation of glass hemisphere SN 6767 in nm.

Lab	1-15 UPR		1-50 UPR		En	
	LSC	U (k = 2)	LSC	U (k = 2)	1-15 UPR	1-50 UPR
Weighted mean	11.840	2.76	13.240	2.87	-	-
NMIJ-1	11.5	8.3	12.5	8.3	0.04	0.10
NIMT	15.2	8.0	16.0	8.0	0.45	0.36
NMIA	15.0	10.0	20.0	10.0	0.33	0.71
NMISA	-	-	10.6	15.0	-	0.18
NMC/A*STAR	10.0	6.0	12.0	7.0	0.34	0.19
KRISS	8.9	7.0	9.4	7.0	0.46	0.60
CMS/ITRI	13.6	8.0	16.0	11.0	0.23	0.26
NIM	12.0	6.0	13.0	6.0	0.03	0.05
Rb	0.631	-	0.759	-	-	-
Rb (limit)	1.468	-	1.438	-	-	-

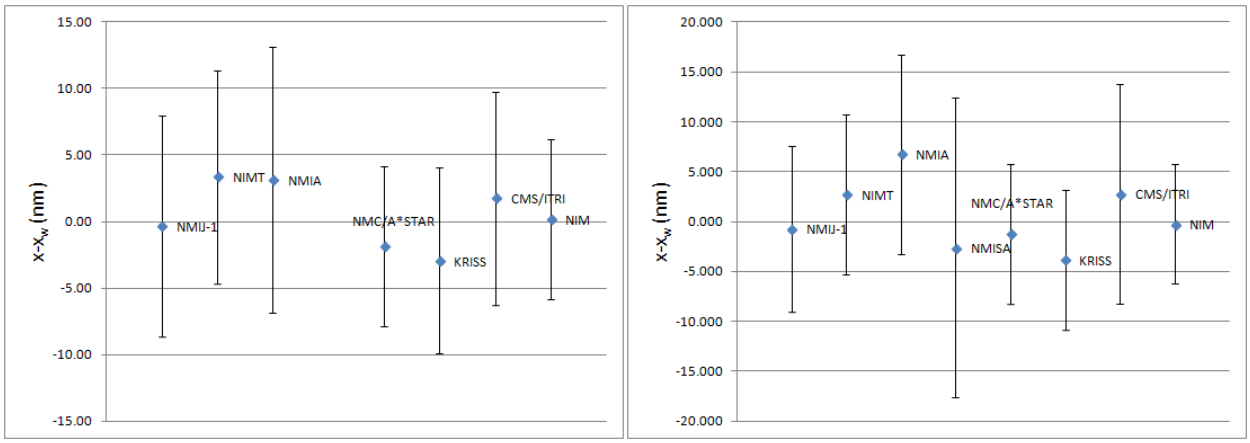

Figure 13: Deviation from SCRV for glass hemisphere SN 6767 at 1-15 UPR and 1-50 UPR.

7.1.3 Harmonic component

High precision roundness measurement for hemi-sphere calibration requires spindle error separation technique, because form error and spindle error are same level. All participants applied multi-step method for spindle error separation in this comparison. In applying multi-step method, it is possible to separate the form error from the spindle error, when number of step is large enough.

In order to determine effect of number of step difference between NMIs, harmonic components of the measurement profile were determined. The calculation results are illustrated in Table 5 and Table 6. For both glass hemispheres (1-50 UPR), dominant components are harmonic at 2^{nd} and 3^{rd} orders. The minimum step performed in error separation process among all participants is 10 steps. Most participants applied 10 or 12 step for multi-step method. NMIJ applied 20 steps. From NMIJ result, amplitude of 10^{th} and 12^{th} components are small. Therefore, it can be assumed that no dominant harmonic was left out during the measurement and analysis process.

The amplitude spectra for the harmonics components are shown in Fig. 14 and Fig. 15. The figure shows similarity of spectra for all participants. Spindle error separation technique of all participants were available, good agreement obtained among the participants.

Table 7. Amplitude (in nm) of each harmonic component of glass hemisphere SN 8726 (1-50 UPR).

Harmonic order	NMIJ-1	NIMT	NMIA	NMISA	NMC/ A*STAR	KRISS	CMS ITRI	NIM	NMIJ-2
1	0.000	0.000	0.000	0.007	0.000	0.000	0.000	0.000	0.000
2	10.110	10.058	11.330	9.663	11.114	11.462	9.954	10.539	10.109
3	1.348	1.018	1.742	1.670	1.539	1.963	1.381	1.560	1.174
4	0.643	1.010	0.943	0.677	1.173	0.862	1.046	0.961	0.933
5	0.540	0.457	0.527	0.287	0.635	0.527	0.524	0.476	0.487
6	0.313	0.343	0.301	0.198	0.307	0.373	0.341	0.112	0.229
7	0.086	0.063	0.288	0.113	0.053	0.186	0.115	0.037	0.212
8	0.065	0.105	0.120	0.085	0.211	0.176	0.137	0.099	0.049
9	0.068	0.012	0.181	0.059	0.165	0.060	0.060	0.140	0.058
10	0.189	0.000	0.265	0.085	0.338	0.121	0.348	0.285	0.288
11	0.070	0.067	0.162	0.034	0.123	0.071	0.010	0.094	0.040
12	0.166	0.188	0.002	0.041	0.653	0.206	0.147	0.096	0.137
13	0.143	0.192	0.198	0.044	0.182	0.224	0.261	0.058	0.169
14	0.138	0.091	0.124	0.042	0.058	0.156	0.065	0.159	0.117
15	0.112	0.236	0.203	0.042	0.203	0.210	0.281	0.227	0.187
16	0.186	0.218	0.136	0.036	0.182	0.131	0.226	0.193	0.158
17	0.110	0.128	0.078	0.010	0.114	0.117	0.104	0.082	0.107
18	0.023	0.051	0.092	0.013	0.128	0.071	0.091	0.086	0.067
19	0.044	0.030	0.026	0.015	0.062	0.051	0.073	0.071	0.048
20	0.000	0.000	0.049	0.013	0.062	0.134	0.048	0.060	0.000

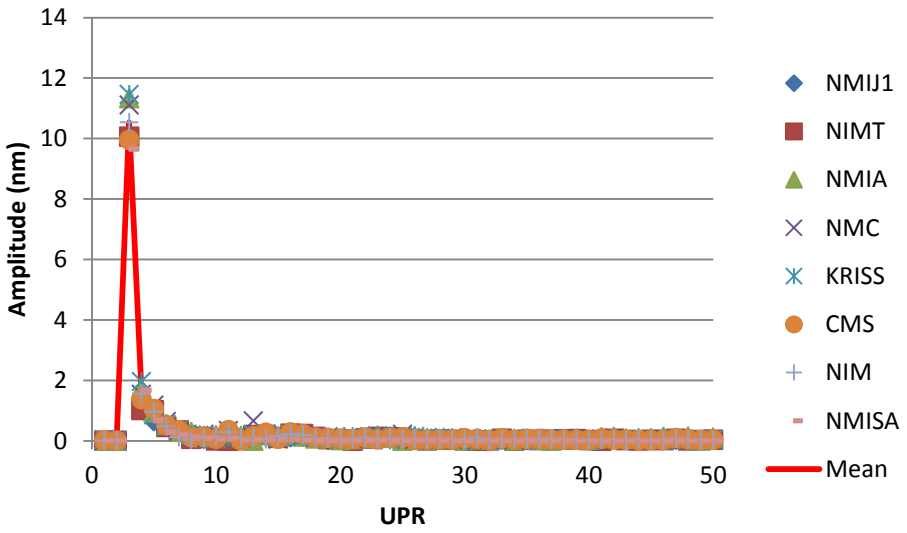

Figure 14: Harmonic component of glass hemisphere SN 8726 (1-50 UPR)**.**

Table 8. Amplitude (in nm) of each harmonic component of glass hemisphere SN 6767(1-50 UPR).

Harmonic order	NMIJ-1	NIMT	NMIA	NMISA	NMC/ A*STAR	KRISS	CMS ITRI	NIM	NMIJ-2
1	0.000	0.000	0.001	0.002	0.000	0.001	0.000	0.000	0.000
2	1.882	2.300	2.786	1.759	1.269	1.415	1.958	1.868	1.861
3	1.008	1.477	1.691	0.907	0.938	0.514	1.282	0.828	0.706
4	0.583	0.692	1.044	0.719	0.636	0.727	0.773	0.901	0.670
5	0.360	0.270	0.475	0.209	0.168	0.257	0.201	0.173	0.351
6	0.341	0.257	0.333	0.072	0.249	0.207	0.301	0.175	0.289
7	0.226	0.173	0.230	0.108	0.164	0.128	0.091	0.089	0.146
8	0.105	0.031	0.082	0.082	0.097	0.090	0.069	0.129	0.091
9	0.112	0.067	0.078	0.058	0.042	0.058	0.158	0.097	0.072
10	0.143	0.000	0.113	0.039	0.128	0.354	0.260	0.194	0.108
11	0.114	0.109	0.093	0.021	0.122	0.072	0.155	0.071	0.094
12	0.169	0.190	0.003	0.042	0.648	0.159	0.194	0.171	0.154
13	0.157	0.131	0.199	0.052	0.106	0.145	0.158	0.102	0.136
14	0.071	0.081	0.051	0.015	0.070	0.035	0.154	0.077	0.070
15	0.047	0.107	0.171	0.016	0.103	0.038	0.089	0.077	0.069
16	0.078	0.106	0.170	0.035	0.049	0.069	0.113	0.072	0.070
17	0.069	0.004	0.050	0.011	0.059	0.062	0.078	0.097	0.067
18	0.032	0.032	0.055	0.009	0.040	0.034	0.140	0.041	0.042
19	0.061	0.087	0.066	0.015	0.099	0.044	0.147	0.024	0.066
20	0.000	0.000	0.082	0.008	0.031	0.004	0.039	0.068	0.000

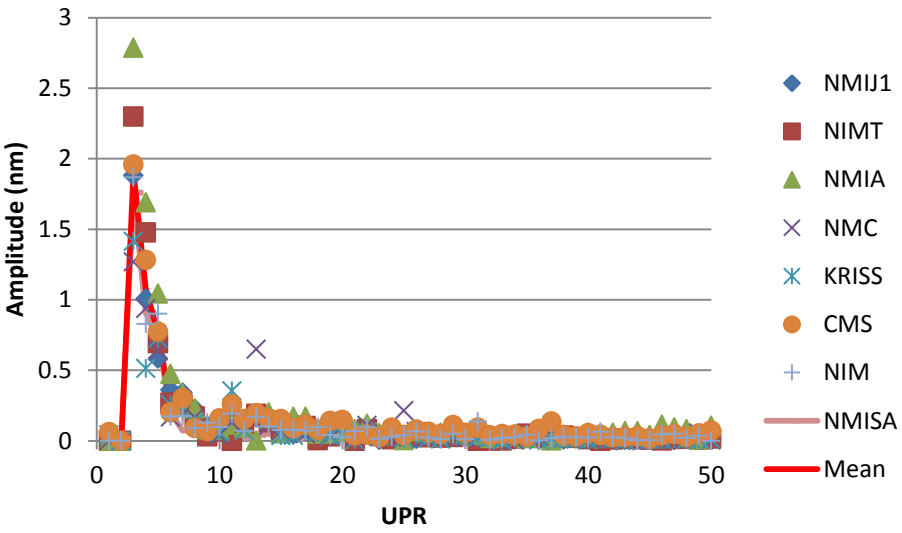

Figure 15: Harmonic component of glass hemisphere SN 6767 (1-50 UPR)**.**

7.1.4 Starting point of profile

In order to compare the measurement condition of participants, the starting point of profile were evaluated. Since the measurand in this comparison was determined from the peak to valley roundness deviation and difference in number of data points of all participants, point to point comparison cannot be conducted. As a result, harmonization of the profile starting points was performed according to paper by H. Haitjema, H. Bosse, M. Frennberg, A. Sacconi and R. Thalman (International comparison of roundness profiles with nanometric accuracy, Metrologia, 33(1996). 67-73). Cross correlation technique was applied where phase shift or measurement starting point can be estimated.

Measured profile of NIMT was used as the reference profile and phase shifting in respect to the reference was estimated. Since there are number of data point difference, linear interpolation was carried out before performing cross correlation. All profiles were normalized by standard deviation of each profiles deviation. The result is shown in Table 9. The objective of this analysis is to determine the variation in phase of the roundness profile.

Table 9. Difference in starting point of the hemisphere profile between each NMIs with NIMT in degree.

Lab	8726_15	8726_50	6767_15	6767_50
NMIJ-1	−5.2	−5.4	1.9	2.6
NIMT	0.0	0.0	0.0	0.0
NMIA	−1.4	−1.8	2.5	3.5
NMISA	−10.7	–	−198.5(−2.2)	–
NMC/A*STAR	−2.1	−2.2	−0.3	−0.9
KRISS	−4.5	−4.5	−1.1	−2.0
CMS ITRI	−0.2	−0.6	2.6	2.4
NIM	−0.7	−0.9	−2.1	−2.1
NMIJ-2	−1.7	−1.6	1.2	1.3

The results in Table 9 clearly show that roundness profile of the artifacts measured by participants have a small deviation in phase which can be due to setup of the measurement and accuracy of the spindle error compensation. Excluding measurement result from NMISA, phase deviation up to 5 degrees was obtained. For glass hemisphere SN 6767, the difference of start points for all participants results are

within several degrees. NMISA of SN 6767 result is larger than other NMIs' result. There are two peaks in cross-correlation function of NMISA SN 6767 profile as shown in Fig. 16. The largest one is at -198.5 degrees and the second one is at -2.2 degrees. It should be noted that the amplitude of peak at -2.2 degrees is almost the same value for all other NMIs' results. In the Fourier component of SN 6767, harmonics components of 2nd and 3rd orders are dominant. Therefore we can see two peaks in cross-correlation function in Fig. 16.

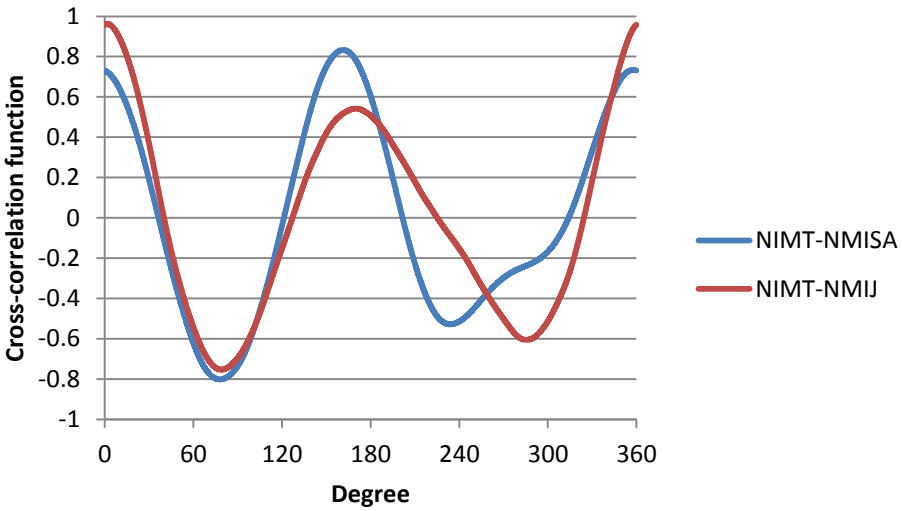

Figure 16: Cross-correlation function between NIMT-NMISA and NIMT-NIMJ**.**

According to Fig. 11, all NMIs except NMISA have the highest peak at approximately at 260 degrees. Whereas, the highest peak of the NMISA's profile is at 70 degrees which is the position of the second highest peak of others profile. Fig. 17 illustrates the roundness profile comparison between NIMT and NMISA and NMIS (phase corrected). Hence, we can conclude that the actual starting point of the NMISA profile for SN 6767 is in fact -2.2 degrees.

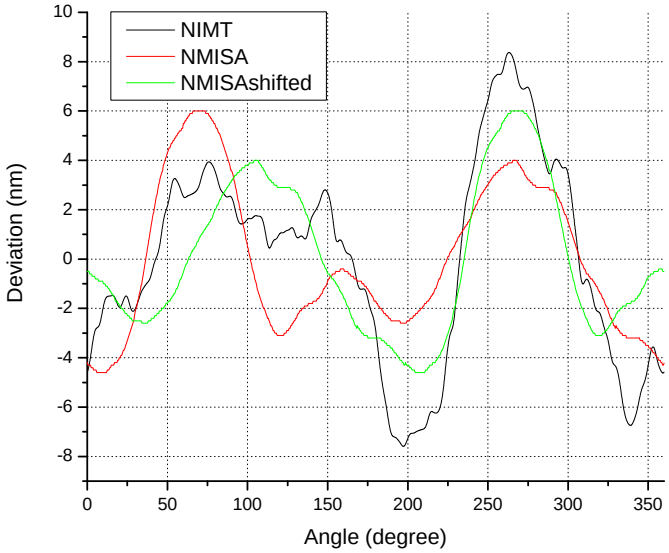

Figure 17: Profile of glass hemisphere SN 6767 at 1-50 UPR of NIMT, NMISA and phase shifted profile of NMISA.

7.2 Softgauges

Softgauges were circulated in numerous formats with seven of the eight laboratories submitting results. Since there is no measurement, only a software output, no uncertainty value is reported. Numerical results of softgauge testing from each laboratory are shown in Table 10. The maximum standard deviation of 0.034 nm was observed which indicates good consistency in filtering algorithm among all participants.

Table 10. Roundness deviation of Softgauge I and Softgauge II.

Lab	Roundness deviation / nm			
	Softgauge I		Softgauge II	
	1-15 UPR	1-50 UPR	1-15 UPR	1-50 UPR
NMIJ	5.79	11.41	8.39	10.88
NIMT	5.80	11.41	8.39	10.88
NMIA	5.7	11.4	8.3	10.9
NMISA	-	-	-	-
NMC/A*STAR	5.78	11.41	8.36	10.89
KRISS	5.78	11.41	8.36	10.88
CMS/ITRI	5.78	11.41	8.36	10.88
NIM	5.8	11.4	8.4	10.9
Average	5.775	11.409	8.364	10.887
σ_{n-1}	0.034	0.006	0.033	0.009

8 Conclusion

Error separation method (multi-step method) was employed in order to achieve high precision roundness measurement of glass hemispheres. Although there are differences in number of step used in error separation method and roundness assessment software used between NMIs, the measurement results are in mutual agreement. The reported results of peak-to-valley departure from roundness are shown in tables 5 and 6. The largest En value was 0.7 for departure from roundness. Upon stability check, both glass hemispheres have no deformation during circulation.

Since numbers of data point of the profile from each NMI are varied, point by point analysis cannot be performed. However, analysis of harmonic component and phase error for all profiles were conducted. A good agreement for harmonic component with deviation within 2 nm was observed.

9 References

[1] ISO 12181-1 Geometrical Product Specifications (GPS) – Roundness – Part 1: Vocabulary and parameters of roundness, International Organization for Standardization, Geneva, Switzerland, 2011.

[2] ISO 12181-2 Geometrical Product Specifications (GPS) – Roundness – Part 2: Specification operators, International Organization for Standardization, Geneva, Switzerland, 2011.

[3] ISO 4291 Methods for the assessment of departure from roundness – Measurement of variations in radius, International Organization for Standardization, Geneva, Switzerland, 1985.

[4] Evaluation of measurement data - Guide to the expression of uncertainty in measurement (GUM), JCGM 100.2008 GUM 1995 with minor corrections, International Organization for Standardization, Geneva, Switzerland, 2008.

[5] ISO/IEC 17043 Conformity assessment – General requirements for proficiency testing, International Organization for Standardization, Geneva, Switzerland, 2010.

[6] M.G. Cox, “The Evaluation of Key Comparison Data”, Metrologia, 2002, 39, 589-595.

[7] H. Haitjema, H. Bosse, M. Frennberg, A. Sacconi, R. Thalmann, “International comparison of roundness profiles with nanometric accuracy”, Metrologia, 1996, 33, 67-73.

[8] H. Bosse, F. Lüdicke, H. Reimann, “An intercomparison on roundness and form measurement”, Measurement, 1994, 13, 107-117.

[9] M. Frennberg, A. Sacconi, “International comparison of high-accuracy roundness measurements”, Metrologia, 1996, 33, 539-544.

[10] EUROMET, “High precision roundness”, Project 533, Final report (Mittatekniikan Keskus, Helsinki, 2001)